

Sarah Ghanbari, Hamideh Vaghari, Zahra Sayyar, Mohammad Adibpour  
and Hoda Jafarizadeh-Malmiri\*

# Autoclave-assisted green synthesis of silver nanoparticles using *A. fumigatus* mycelia extract and the evaluation of their physico-chemical properties and antibacterial activity

<https://doi.org/10.1515/gps-2017-0062>

Received April 24, 2017; accepted May 31, 2017; previously published online August 8, 2017

**Abstract:** Silver nanoparticles (AgNPs) were synthesized using *Aspergillus fumigatus* (*A. fumigatus*) mycelia extract via the hydrothermal method. The main reducing and stabilizing groups and components of *A. fumigatus* extract, such as amine, hydroxyl, amid, protein, enzymes, and cell saccharide compounds, were identified by Fourier transform infrared (FT-IR). Central composition design was used to plan the experiments, and response surface methodology was applied to evaluate of the effects of independent variables, including the amount of the prepared extract (5–7 ml) and heating time (10–20 min) at 121°C and 1.5 bar), on the particle size of the synthesized AgNPs, as manifested in broad emission peak ( $\lambda_{\text{max}}$ ). More stable and spherical monodispersed AgNPs, with mean particle size, polydispersity index (PDI) value, and maximum  $\zeta$  potential value of 23 nm, 0.270, and +35.3 mV, respectively, were obtained at the optimal synthesis conditions using 7 ml of *A. fumigatus* extract and heating time of 20 min. The synthesized AgNPs indicated high antibacterial activity against both Gram-positive and Gram-negative bacteria.

**Keywords:** antibacterial activity; *Aspergillus fumigatus*; green synthesis; response surface methodology; silver nanoparticles.

## 1 Introduction

The biosynthesis of metal and metal oxide nanoparticles (NPs) using biological resources has gained great research

attention due to its green and eco-friendly nature. As compared with the variety of chemical and physical procedures that can be used in the synthesis of inorganic NPs, green synthesis processes have attracted great interest because they do not use toxic solvents, do not generate hazardous by-products, and consume high energy [1, 2]. An enormous group of biological resources, such as plant extracts, algae, fungi, yeast, bacteria, and viruses, available in nature can be used in NPs synthesis [3]. Several studies have indicated that both unicellular and multicellular organisms have intracellular or extracellular potential for inorganic NPs synthesis [4, 5].

Recent studies have reported that fungi show good potential for synthesizing NPs when compared with other microorganisms [6–9]. In fact, fungi have a good potential to easily produce extra cellular enzymes in large amounts, which can reduce metal ions and fabricate metal NPs. Furthermore, the presence of proteins in the spent medium of the fungi has been found to be responsible for the stabilizing and capping properties of the synthesized NPs [10]. Filamentous fungi play an important role in the NPs biosynthesis. The extracellular biosynthesis of NPs using filamentous fungi, such as *Aspergillus fumigatus*, is rapid and makes downstream processing much easier [4, 8]. *A. fumigatus* has been successfully used to synthesis silver nanoparticles (AgNPs) [4, 6, 10]. Results indicated that the synthesis of AgNPs using this fungus is quicker compared with the chemical and physical methodsof AgNPs synthesis. Therefore, *A. fumigatus* can be used in fabricating large amounts of AgNPs.

In nanobiotechnology research, AgNPs have received much attention due to their unique physical, chemical, and biological properties. AgNPs are effective against pathogenic microbes and are known as efficient antimicrobial agents. AgNPs also have excellent antifungal and antiviral properties, thus increasing their possible applications in diverse areas, such as cosmetics, coatings, food packaging, and medicine [5, 11, 12]. In the biological synthesis of AgNPs, successfully controlling average particle size range and uniform particle morphology is more important. These properties can be affected by reaction conditions, such as pH, temperature, and the proportion of salts/reducing agent [10].

\*Corresponding author: Hoda Jafarizadeh-Malmiri, Faculty of Chemical Engineering, Sahand University of Technology, 51335-1996 Sahand, Tabriz, Iran, e-mail: h\_jafarizadeh@sut.ac.ir

**Sarah Ghanbari:** Faculty of Biotechnology, Higher Education of Rab-Rashidi, Tabriz, Iran

**Hamideh Vaghari and Zahra Sayyar:** Faculty of Chemical Engineering, Sahand University of Technology, 51335-1996 Sahand, Tabriz, Iran

**Mohammad Adibpour:** Faculty of Medicine, Tabriz University of Medical Science, Tabriz, Iran

Therefore, the main objectives of the present study were to (i) analyze and use aqueous *A. fumigatus* extract for AgNPs synthesis, (ii) find the optimal reduction conditions to synthesize AgNPs with minimum mean particle size and maximum stability over time using fungal extract, and (iii) evaluate the antibacterial activities of the synthesized AgNPs.

## 2 Materials and methods

### 2.1 Materials

Silver salt ( $\text{AgNO}_3$ ) was purchased from Dr. Mojallali (Dr. Mojallali Chemical Complex Co. Tehran, Iran). Standard solution of AgNPs (with particle size of 10 nm and concentration of 1000 ppm) was obtained from Tecnan-Nanomat (Navarra, Spain).

*Aspergillus fumigatus* (PTCC 5009) was purchased from microbial Persian type culture collection (PTCC, Tehran, Iran). Potato dextrose agar (PDA) and potato dextrose broth (PDB) as culture media were provided from Oxoid (Oxoid Ltd., Hampshire, England) and Biomark (Biomark Inc. Richmond, Canada). *Escherichia coli* (PTCC 1395) and *Staphylococcus aureus* (PTCC 1189) were provided from microbial PTCC (Tehran, Iran). Nutrient agar (NA) was purchased from Biolife (Biolife Co. Milan, Italy). Deionized double-distilled water was used in preparing all aqueous solutions.

### 2.2 Preparation of *A. fumigatus* mycelia extract

*A. fumigatus* was cultured on PDA for 7 days at 25°C. After incubation, the fungal spores were isolated, and fungal spore suspension containing  $10^6$  spores/ml was prepared. Spore concentration of spore suspension was evaluated by using a Neubauer's chamber (haemocytometer), according to the classical procedure. About 1 ml of the provided spore suspension was added into the 100 ml of the PDB and incubated in a shaker incubator (New Brunswick Scientific, Innova 4000, NJ, USA) for 4 days (120 rpm and 25°C). In order to remove any medium traces, the fungal mycelia was separated by filtering through Whatman filter paper No. 1 and then washed thrice with sterile distilled water. Separated wet mycelia was added into 100 ml sterile double distilled water and placed in shaker incubator (120 rpm and 25°C) for 3 days. The mixture was then centrifuged (Sigma 3-18K, Gottingen, Germany) for 5 min at 6500 rpm and filtered through a 0.2  $\mu\text{m}$  micro filter. The filtered *A. fumigatus* mycelia extract was stored in the refrigerator at 4°C.

### 2.3 Synthesis of AgNPs using *A. fumigatus* mycelia extract

According to the literature, silver nitrate solution (1 mM) was prepared by dissolving 0.017 g of its powder in 100 ml of DI water [11, 13, 14]. Different amounts (5–7 ml) of provided mycelia extract with 3 ml of  $\text{AgNO}_3$  solution was mixed, after which the mixture solutions were kept in autoclave at 15 psi pressure and 121°C for different times (10–20 min).

### 2.4 Analysis

**2.4.1 *A. fumigatus* mycelia extract:** The contributions of the possible functional groups in *A. fumigatus* mycelia extract for the formation of AgNPs were evaluated using Fourier transform-infrared spectroscopy (FT-IR) analysis. The FT-IR spectra of *A. fumigatus* mycelia extract were recorded on a Bruker Tensor 27 spectrometer (Bruker, Germany) using KBr pellets in the 4000–400  $\text{cm}^{-1}$  region.

**2.4.2 Synthesized AgNPs:** The formation of AgNPs was monitored at regular intervals by scanning the reacting mixture under a spectrophotometer due to their surface plasmon resonance (SPR). In order to characterize SPR of AgNPs solutions, the absorption spectra of the solutions were taken with a UV-Vis spectrophotometer using a Jenway UV-Vis spectrophotometer 6705 (UK) in a 1 cm optical path quartz cuvette. As can be observed, the broad emission peaks ( $\lambda_{\text{max}}$ ) are centered (380–450 nm) due to the excitation of surface plasmon vibration bands, and this is responsible for the striking yellow-brown color of AgNPs in various media [15].

UV-Vis spectroscopy measurements can also be used to evaluate the concentration of AgNPs solution. In fact, the absorbance of the AgNP solution is proportional to the concentration of formed AgNPs. To measure the concentration of synthesized AgNPs, the standard curve was established using several serial dilute solutions of AgNPs (10–1000 ppm) from the standard solution of AgNPs (1000 ppm). The concentration of the sample was obtained by comparing the absorbance of the synthesized NPs with the standard curve.

A dynamic light scattering (DLS) particle size analyzer (Nanotrac Wave, Microtrac, USA) was utilized to estimate the particle size, particle size distribution (PSD), Polydispersity index (PDI) and  $\zeta$  potential values of the synthesized AgNPs.

The morphological evaluation of the synthesized AgNPs was performed by transmission electron microscopy (TEM, CM120, Philips, Amsterdam, Netherlands) with an acceleration voltage of 120 kV. For the TEM measurements, a drop of solution containing AgNPs was deposited on a carbon-coated copper grid.

Well diffusion method was carried out to examine the antibacterial activities of the synthesized AgNPs. In fact, 0.1 ml of the provided bacterial suspensions adjusted to 0.5 McFarland standard, containing  $1.5 \times 10^8$  colony forming units of bacteria in 1 ml of prepared suspensions, were inoculated on NA culture media at the plates (90 ml in diameter), after which some holes (with diameter of 5 mm) were created in the inoculated culture media. Next, 10  $\mu\text{l}$  of the synthesized AgNPs solutions were poured into each hole. The provided plates were then placed in the incubator at 37°C for 24 h.

### 2.5 Experimental design and statistical analysis

Central composite design (CCD) with two independent synthesized variables, namely, amount of *A. fumigatus* mycelia extract (5–7 ml) ( $X_1$ ) and autoclaved heating time (10–20 min) ( $X_2$ ), was applied to the design of experiments using the software Minitab v.16 statistical package (Minitab Inc., PA, USA). Response variables were chosen according to the literature [6, 10]. Therefore, 13 experiment runs, including 4 factorial points, 4 star points, and 5 central points, were generated (Table 1) and carried out in 1 day (one block) [16]. In order to estimate the pure error, a central point ( $X_1$ : 6 ml and  $X_2$ : 15 min) was repeated for five times [17]. Response surface methodology (RSM)

**Table 1:** Central composite design and response variables for the final model.

Experiment no.	Amount of fungal mycelia extract (ml)	Heating time (min)	$\lambda_{\max}$ (nm)	
			Experimental	Predicted
1	5	15	480	470
2 (C)	6	15	470	470
3 (C)	6	15	465	470
4	5.3	18.5	469	472
5 (C)	6	15	476	470
6 (C)	6	15	468	470
7	6.7	11.5	465	465
8	6	20	454	452
9 (C)	6	15	473	470
10	7	15	436	437
11	6	10	482	481
12	5.3	11.5	475	478
13	6.7	18.5	468	431

C, Center point.

was used to evaluate the effects of the independent variables on the response variable, namely,  $\lambda_{\max}$  (Y, nm) of the synthesized AgNPs. The  $\lambda_{\max}$  (broad emission peak) can be correlated to the particle size of the formed NPs as the longer wavelengths correspond to an increase in particle size [18].

A second-order polynomial equation (Eq. 1) was used to correlate the response variables to the studied synthesized variables

$$Y = A_0 + A_1 X_1 + A_2 X_2 + A_{11} X_1^2 + A_{22} X_2^2 + A_{12} X_1 X_2, \quad (1)$$

where Y is the response variable,  $A_0$  is a constant,  $A_1$  and  $A_2$  correspond to the linear terms,  $A_{11}$  and  $A_{22}$  represent the quadratic terms, and  $A_{12}$  indicates the interaction terms. The suitability of the model was studied while considering the coefficient of determination ( $R^2$ ) and adjusting the coefficient of determination ( $R^2\text{-adj}$ ). Analysis of variance (ANOVA) was also carried out to provide the significance determinations of the resulted models in terms of p-value and F ratio. High values of F ratio and small p-value ( $<0.05$ ) were considered as statistically significant. Based on the fitted polynomial equations, a three-dimensional surface plot was designed to better visualize the independent variable interaction [19]. In order to obtain the optimum levels of independent synthesized variables with the desired response variables, numerical response optimization and graphical optimization using a two dimensional contour plot were applied [20]. For verifying the validity of the statistical experimental approaches, three additional approval tests were performed at the obtained optimum synthesis conditions.

### 3 Results and discussion

#### 3.1 Characterization of the *A. fumigatus* mycelia extract

As clearly observed in the FT-IR spectra of the *A. fumigatus* mycelia (Figure 1), three main absorption peaks were

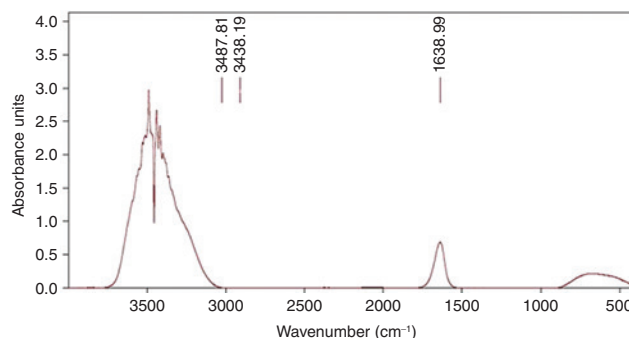


**Figure 1:** FT-IR spectra of *A. fumigatus* mycelia extract.

centered at 1638.99, 3438.19, and 3487.81  $\text{cm}^{-1}$  which were in the region range of 400–4000  $\text{cm}^{-1}$ . The most wide spectra absorption peaks were observed at 3487.81 and 3438.19  $\text{cm}^{-1}$ , which can be attributed to the stretching vibrations of the OH (hydroxyl groups) of saccharides in the fungal cell wall [21]. Furthermore, the peak at 3438.19  $\text{cm}^{-1}$  indicated N-H stretching vibrations in amide linkages of proteins. The band at 1638.99  $\text{cm}^{-1}$ , referring to the carbonyl stretch, was assigned to the amide I bond of protein. The results indicated that the presence of the proteins and enzymes can reduce the  $\text{Ag}^+$  ions to atoms and form AgNPs. It seems that the main possible mechanism for the formation of AgNPs by the *A. fumigatus* mycelia extract is through the nitrate reductases. The obtained results are in agreement with findings of Phanom and Ahmed [22], who reported that nitrate reductase of *A. oryzae* is the main reducing agent in the synthesis of AgNPs. Meanwhile, the presence of proteins in *A. fumigatus* mycelia extract may have been responsible for stabilizing the synthesized NPs [10].

#### 3.2 Fitting the response surface models

According to the design of experiments, second-order polynomial models were fitted using the response variables obtained from the experimental runs (Table 1). The predictable regression coefficients and the corresponding significance of regressions for the model are given in Table 2. The F ratio and p-values of the all terms in obtained model, which are used to evaluate their effectiveness, are also shown in Table 3.

Given that the overall model performance could be manifested in coefficients of determinations, the resulting quite high values for  $R^2$  (0.938) and  $R^2\text{-adj}$  (0.862) verified the fitness of the proposed model. Moreover, the achieved non-significant lack of fit for the proposed final model ( $p > 0.05$ ) confirmed its sufficient fitness to the synthesis

**Table 2:** Regression coefficients ( $R^2$ ), adjusted  $R^2$  ( $R^2$ -adj), and probability values for the model.

Regression coefficient <sup>a</sup>	Clear zone area (mm <sup>2</sup> )
$\beta_0$ (constant)	-162.946
$\beta_1$ (main effect)	190.231
$\beta_2$ (main effect)	19.020
$\beta_{11}$ (quadratic effect)	-13.009
$\beta_{22}$ (quadratic effect)	-0.156
$\beta_{12}$ (interaction effect)	-2.861
$R^2$	0.938
$R^2$ -adj	0.862
Lack of fit (p-value)	0.586

<sup>a</sup> $\beta_0$  is a constant;  $\beta_1, \beta_{11}$  and  $\beta_{22}$  are the linear, quadratic, and interaction coefficients of the quadratic polynomial equation, respectively.

1, Amount of utilized fungal mycelia extract solution (ml); 2, heating time (min).

**Table 3:** Significance probability (p-value, F ratio) of regression coefficients in the second-order polynomial model.

Main effects	Main effects		Quadratic effects		Interacted effects
	$X_1$	$X_2$	$X_1^2$	$X_2^2$	
Clear zone area (mm <sup>2</sup> )					
p-Value	0.032	0.129 <sup>a</sup>	0.034	0.426 <sup>a</sup>	0.045
F ratio	10.52	3.64	9.94	0.78	7.86

<sup>a</sup>Not significant ( $p > 0.05$ ).

1, Amount of utilized fungal mycelia extract solution (ml); 2, heating time (min).

parameter effects (Table 2). As clearly observed in Table 3, the main and quadratic effects of heating time had non-significant ( $p > 0.05$ ) effects on the  $\lambda_{\max}$  (particle size) of the synthesized AgNPs. However, its interaction with the amount of the *A. fumigatus* mycelia extract had a significant effect on the  $\lambda_{\max}$  of the synthesized AgNPs.

### 3.2.1 $\lambda_{\max}$ of the synthesized AgNPs

The  $\lambda_{\max}$  of the obtained AgNPs ranged from 436 to 482 nm (Table 1). In fact, the particle size of synthesized AgNPs can be manifested in the  $\lambda_{\max}$  of the AgNPs. Generally, the longer wavelengths in the absorption spectra of metal NPs are correlated to their bigger size [23]. The  $\lambda_{\max}$  of the synthesized AgNPs as a function of *A. fumigatus* mycelia extract and autoclaved heating time is shown in Figure 2. As clearly observed in the figure, at constant heating time, the  $\lambda_{\max}$  of the synthesized AgNPs decreased when the amount of mycelia extract increased. The obtained result

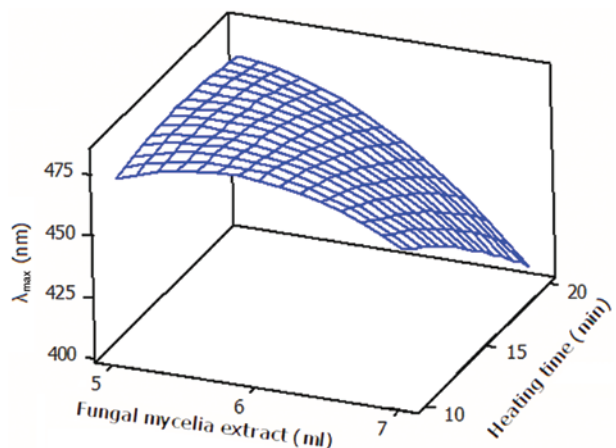


**Figure 2:** Surface plot for  $\lambda_{\max}$  of the synthesized AgNP solution as a function of the *A. fumigatus* mycelia extract and heating time.

can be explained by the fact that increasing the amount of fungal extract increased the concentration of its reducing molecule (nitrate reductase) and stabilizing agents (sugars and proteins), which in turn, stabilized the molecules, thus creating a layer around the synthesized AgNPs and decreasing AgNP agglomeration [1, 2]. The results also indicated that at higher amount of fungal extract, the  $\lambda_{\max}$  of the synthesized AgNPs decreased when the heating time increased. However, at a lower amount of mycelia extract, heating time did not show a significant ( $p < 0.05$ ) effect on the  $\lambda_{\max}$  of the formed AgNPs. It seems that by increasing the heating time, the moving speed of the formed AgNPs in the solution was enhanced, which in turn, increased the collision frequency between NPs increased and resulted in their decreased particle size [2]. The presence of a slight curvature in the  $\lambda_{\max}$  curve (Figure 2) confirmed the significant effects of the amount of *A. fumigatus* mycelia extract and autoclaved heating time.

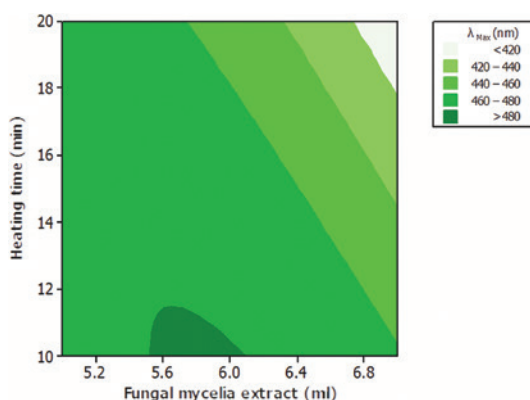


**Figure 3:** Contour plot for  $\lambda_{\max}$  of the synthesized AgNP solution as a function of the *A. fumigatus* mycelia extract and heating time.

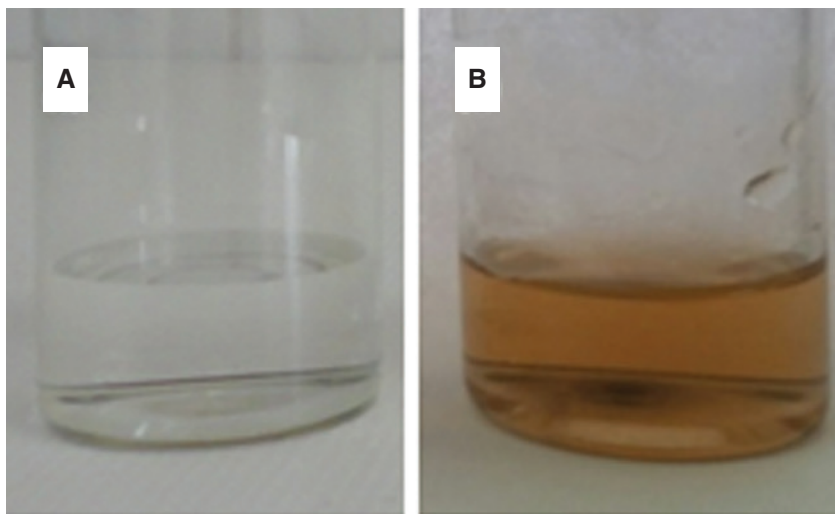


**Figure 4:** Color and appearance of the mixture solution containing  $\text{AgNO}_3$  and *A. fumigatus* mycelia extract (A) at the beginning of heating and (B) after heating and subsequent formation of AgNPs.

### 3.3 Optimization of processing parameters for the synthesized AgNPs

The optimum conditions for AgNPs synthesis can be achieved when the process resulted in the formation of the smallest mean particle size ( $\lambda_{\max}$ ). Graphical optimization based on a contour plot was used to find the optimum region for the synthesis parameters to produce AgNPs with the minimum particle size (Figure 3). As clearly observed in Figure 3, the minimum  $\lambda_{\max}$  for the synthesized AgNPs was obtained at a higher heating time and higher amount of *A. fumigatus* mycelia extract.

Numerical optimization was also used to determine the optimum levels of the studied variables. The results suggested that the synthesis conditions with 7 ml of fungal mycelia solution and 20 min of autoclaved heating time generated the most desirable AgNPs with  $\lambda_{\max}$  of 404.45 nm. Moreover, three AgNPs solutions were prepared according to the recommended optimal levels by numerical optimization and were characterized in terms of the  $\lambda_{\max}$ . The measured experimental value for the  $\lambda_{\max}$  of these three AgNPs solutions was obtained at  $407 \pm 3$  nm. The non-significant differences found between the predicted and experimental values of the synthesized AgNPs at optimum synthesized conditions indicated the adequacy of the obtained and fitted model by RSM.

### 3.4 Specifications of the synthesized AgNPs at obtained optimum conditions

The appearance of brownish color proved that the AgNPs formed in the reaction mixture solution as a result of

the reduction of the  $\text{Ag}^+$  to Ag. Figure 4 indicates the color change of the mixture solution containing  $\text{AgNO}_3$  and *A. fumigatus* mycelia extract at the beginning of the reaction (heating) and after heating and formation of AgNPs. The obtained result is in agreement with the finding of Bhainsa and D'Souza [24], who observed the brownish color of AgNP solution synthesized using *A. fumigatus* extract. The color change occurred due to the

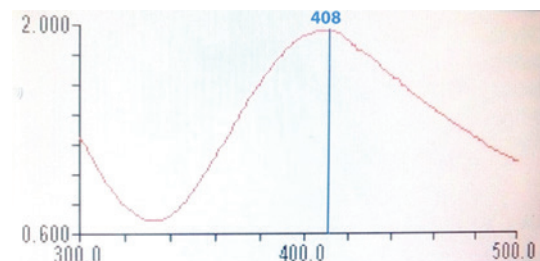


**Figure 5:** Surface plasmon resonance spectrum of the synthesized AgNPs at obtained optimum synthesis conditions.

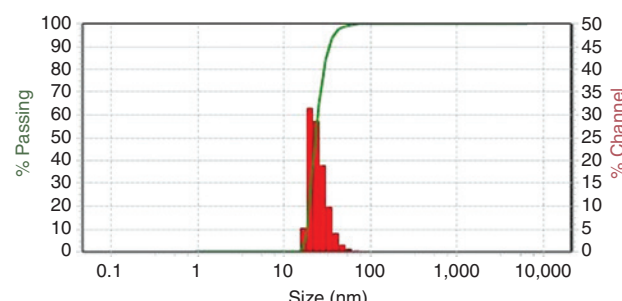


**Figure 6:** Particle size distribution of the synthesized AgNPs at obtained optimum synthesis conditions.

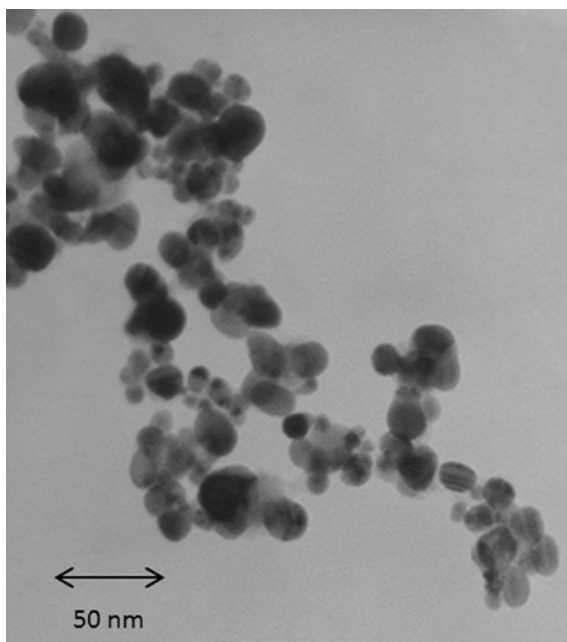


**Figure 7:** TEM image of the synthesized AgNPs at obtained optimum conditions.

surface plasmon resonance (SPR) of the formed AgNPs (Figure 5). As clearly observed in Figure 4,  $\lambda_{\max}$  of the synthesized AgNPs was obtained at 407 nm, which was in the favorable range for AgNPs (380–450 nm) [15]. The obtained result indicated that the concentration of AgNP synthesized solution obtained at optimum condition was 65 ppm.

The particle size of the synthesized AgNPs ranged between 18 and 40 nm with an average size of 23 nm. Figure 6 indicates the particle size distribution of the synthesized AgNPs. The PDI and  $\zeta$  potential values of the synthesized AgNPs using *A. fumigatus* mycelia extract at obtained optimum synthesized conditions were 0.270 and +35.3 mV, respectively. The obtained results indicated that

the more stable AgNPs formed at the optimum synthesized conditions, which were covered with a thin layer of proteins comprising positively charged groups (NH). The obtained results are in agreement with the results of the FT-IR analysis.

A typical TEM image of the synthesized AgNPs is shown in Figure 7. As clearly observed, the synthesized NPs were well dispersed with spherical structures; in fact, spherical NPs were more abundant than NPs of other shapes. This spherical shape indicated that the synthesized NPs had minimum surface energy and high thermodynamic stability, thus confirming the high value of the  $\zeta$  potential of the synthesized AgNPs.

### 3.5 Antibacterial activity of the synthesized AgNPs at obtained optimum conditions

The antibacterial activity of synthesized AgNPs on the growth of Gram-positive (*S. aureus*) and Gram negative (*E. coli*) bacteria during incubation are shown in Figure 8. As can be seen in the figure, the zones of inhibition were observed with *S. aureus* (11 mm) and *E. coli* (9 mm). The obtained results are in agreement with the findings of Ratnasri and Hemalatha [25], and Bala and Arya [26], who found that the synthesized AgNPs using *A. fumigatus* have strong antibacterial activities against both Gram-positive and Gram-negative bacteria species.

## 4 Conclusions

Green approaches of AgNPs synthesis using microorganisms are cheap, simple, completely safe, and environment-friendly. In fact, the synthesis of NPs from the



**Figure 8:** Created zones of inhibition with (A) *S. aureus* and (B) *E. coli* incubated at 37°C for 24 h.

microbes enhanced advance research in nanotechnology. However, due to their relatively high titrate reductases content, fungi are much preferable in the synthesis of metal NPs as compared with the bacteria species. The filamentous fungus, *A. fumigatus*, has shown potential for extracellular synthesis of more stable AgNPs with small particle sizes and high antibacterial activities. RSM was successfully applied to develop an empirical model (1) to predict the particle size ( $\lambda_{\max}$ ) of the synthesized AgNPs as a function of *A. fumigatus* mycelia extract and reaction heating time and (2) to optimize the synthesis parameters. The developed AgNPs synthesis method from the present study can be used widely in the synthesis of other noble metal NPs.

**Acknowledgments:** The authors would like to thank the Food Engineering Research Institute of the Sahand University of Technology for supporting the development of an innovative methodology for the safe assessment of industrial nanomaterials.

## References

- [1] Mohammadalou M, Jafarizadeh-Malmiri H, and Maghsoudi H. *Green Process. Synth.* 2017, 6, 31–42.
- [2] Eskandari-Nojedehi M, Jafarizadeh-Malmiri H, Rahbar-Shahrouzi J. *Nanotechnol. Rev.* 2016, 5, 537–548.
- [3] Thakkar KN, Mhatre SS, Parikh, RY. *Nanomedicine* 2010, 6, 257–262.
- [4] Hulkoti NI, Taranath TC. *Colloids Surf. B* 2014, 121, 474–483.
- [5] Mohammadalou M, Maghsoudi H, Jafarizadeh-Malmiri H. *Int. Food Res. J.* 2016, 23, 446–463.
- [6] Alani F, Moo-Young M, Anderson W. *World J. Microbiol. Biotechnol.* 2012, 28, 1081–1086.
- [7] Rajakumar G, Abdul Rahuman A, Mohana Roopan S, Gopiesh Khanna V, Elango G, Kamaraj C, Abduz Zahir A, Velayutham K. *Spectrochim. Acta Mol. Biomol. Spectrosc.* 2012, 91, 23–29.
- [8] Gupta S, Bector S. *Antonie van Leeuwenhoek* 2013, 103, 1113–1123.
- [9] Raliya R, Tarafdar JC. *Int. Nano Lett.* 2014, 4, 1–10.
- [10] Quester K, Avalos-Borja M, Castro-Longoria E. *J. Biomater. Nanobiotechnol.* 2016, 7, 118–125.
- [11] Okafor F, Janen A, Kukhtareva T, Edwards V, Curley M. *Int. J. Environ. Res. Public Health* 2013, 10, 5221–5238.
- [12] Vivek R, Thangam R, Muthuchelian K, Gunasekaran P, Kaveri K, Kannan S. *Process Biochem.* 2012, 47, 2405–2410.
- [13] Njagi EC, Huang H, Stafford L, Genuino H, Galindo HM, Collins JB, Hoag GE, Suib SL. *Langmuir*. 2010, 27, 264–271.
- [14] Li S, Shen Y, Xie A, Yu X, Qiu L, Zhang L, Zhang Q. *Green Chem.* 2007, 9, 852–858.
- [15] Han JW, Gurunathan S, Jeong JK, Choi YJ, Kwon DN, Park JK, Kim JH. *Nanoscale Res. Lett.* 2014, 9, 459.
- [16] Jafari N, Jafarizadeh-Malmiri H, Hamzeh-Mivehroud M, Adib-pour M. *Green Process. Synth.* 2017, 6, 333–340.
- [17] Ahdno H, Jafarizadeh-Malmiri H. *Food Bioprod. Process* 2017, 101, 193–204.
- [18] Eskandari-Nojedehi M, Jafarizadeh-Malmiri H, Rahbar-Shahrouzi J. *Green Process. Synth.* doi: 10.1515/gps-2017-0004.
- [19] Anarjan N, Jafarizadeh-Malmiri H, Nehdi IA, Sbihi HM, Al-Resayes SI, Tan CP. *Int. J. Nanomed.* 2015, 10, 1109–1118.
- [20] Anarjan N, Jafarizadeh-Malmiri H, Ling TC, Tan CP. *Int. J. Food Prop.* 2014, 17, 937–947.
- [21] Sabatini L, Battistelli M, Giorgic L, Iacobucci M, Gobbid L, Andreozzi E, Pianetti A, Franchi R, Bruscolini F. *Materials* 2016, 306, 115–123.
- [22] Phanom A, Ahmed G. *Nanosci. Nanotechnol.* 2015, 5, 14–21.
- [23] Kannan N, Mukunthan K, Balaji S. *Colloids Surf. B. Biointerfaces.* 2011, 86, 378–383.
- [24] Bhainsa KC, D'Souza SF. *Colloid Surf. B. Biointerfaces.* 2006, 47, 160–164.
- [25] Ratnasi PV, Hemalatha KPJ. *Am. J. Adv. Drug Deliv.* 2014, 2, 741–751.
- [26] Bala M, Arya V. *Int. J. Nanomater. Biostruct.* 2013, 3, 37–41.

## Bionotes

Sarah Ghanbari



Sarah Ghanbari obtained her BSc degree in Cell and Molecular Sciences (2013) and her MSc degree in Microbial Biotechnology (2016) from the Higher Education Institute of Rab-Rashid, Iran. The present study is part of the results of her Master's thesis, which she completed under the supervision of Associate Profesor Dr. Hoda Jafarizadeh-Malmiri. Her field of interest is nanobiotechnology, in particular green synthesis of metal nanoparticles using microorganisms and evaluation of their antimicrobial activities.

Hamideh Vaghari



Hamideh Vaghari obtained her BSc degree in Applied Chemistry from Islamic Azad University of Tabriz, Iran. She obtained her MSc degree in Biotechnology from Sahand University of Technology in 2014. Her MSc thesis was related to lipid accumulation in the local species of *Dunaliella salina* for biodiesel production on a pilot scale, which was done under the supervision of Associate Profesor Dr. Hoda Jafarizadeh-Malmiri. Her fields of interest include food biotechnology and nanobiotechnology.

**Zahra Sayyar**

Zahra Sayyar obtained her BSc degree in Petrochemical Engineering from Sahand University of Technology (SUT), Iran. For her Bachelor's thesis, she focused on industrial waste water treatment by advanced oxidation. She obtained her MSc degree in Chemical Engineering from SUT in 2013. She worked on self-cleaning surfaces (nanotechnology). Presently, she is a PhD student at SUT (supervisor: Associate Professor Hoda Jafarizadeh-Malmiri). Her field of interest includes nanoemulsion formation and the evaluation of its bioavailability.

**Hoda Jafarizadeh-Malmiri**

Hoda Jafarizadeh-Malmiri received his BSc and MSc degrees in Food Engineering (Iran). He obtained his PhD in Food Science from Universiti Putra, Malaysia in 2012. His PhD thesis was on extension of shelf life of banana using edible coating conjugated with silver nanoparticles. He joined Sahand University of Technology, Iran in 2012 and is currently working as an associate professor in the Faculty of Chemical Engineering. He is the head of the Food Research Institute. His fields of interest include nanobiotechnology, food biotechnology, green processes, and organic and inorganic nanoparticles synthesis.

**Mohammad Adibpour**

Mohammad Adibpour received his Bachelor's degree in Laboratory Sciences from Tabriz University of Medical Sciences in 1990. He obtained his Master's degree in the field of Medical Mycology from Tehran University of Medical Sciences (1993). His MSc thesis concentrated on studying cortisol in patients with tinea versicolor. In 1993, he was hired as a member of the Faculty of Medicine, Tabriz University of Medical Sciences. Presently, he is working as an instructor at the School of Medicine. His research fields include diagnosis of yeast-like fungi, infectivity of yeast-like mouth disease, and nanoparticle synthesis using fungi.